Engineering Structures 289 (2023) 116220

Contents lists available at ScienceDirect

Engineering Structures

journal homepage: www.elsevier.com/locate/engstruct

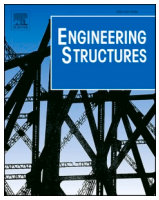

Fragility assessment of traditional wooden houses in Madagascar subjected to extreme wind loads

Rafik Taleb [a,b,*], Harinaivo Ramanantoa [c], Thomas Reynolds [a], Christopher T.S. Beckett [a], Yuner Huang [a], Malalatiana Rakotoarivony [d], Alexandre S. Gagnon [e], Luciano Andriamaro [d]

[a] School of Engineering, University of Edinburgh, King's Buildings, Edinburgh EH9 3FB, UK
[b] Department of Civil Engineering, University of Blida 1, BP270 Blida, Algeria
[c] University Magis, BP 3832, Amparibe, Antananarivo, Madagascar
[d] Conservation International – Madagascar, B.P. 5178 Antananarivo (101), Madagascar
[e] School of Biological and Environmental Sciences, Liverpool John Moores University, Byrom Street, Liverpool L3 3AF, UK

ARTICLE INFO

Keywords:
Cyclones
Fragility analysis
Madagascar
Traditional wooden houses
Wind load

ABSTRACT

Cyclones are a common hazard in Madagascar, each year causing fatalities and damage to the physical and socioeconomic infrastructure. Residential infrastructures are a critical sector within the built environment and studying their performance under natural hazards is a significant step for assessing the risk and resilience of a community. In the coastal regions of Madagascar, more than 80% of houses are self-built, non-engineered traditional wooden houses constructed based on heritage practices and using low or no-cost materials collected in nearby areas or forests. These traditional wooden houses are particularly vulnerable to cyclonic winds, and in this paper, a novel approach is used to evaluate their structural performance and to predict their likelihood of failure under extreme wind conditions. The structural systems and their damage due to extreme winds were first evaluated based on field surveys and collected information such as post-disaster reports. A range of field tests was then carried out at two coastal sites to evaluate the strength of the members and connections identified as commonly used for constructing traditional wooden houses in Madagascar. Damage fragility curves were subsequently developed based on the performance of the connections of roof coverings, wall claddings, the roof structural system, and the performance of columns embedded into the ground and combined to predict the structure's performance. The experimental methods and results presented in this study can be exploited to improve the existing Malagasy guidelines for cyclone resistance of traditional wooden houses published in 2016. The developed fragility curves can also be used to represent traditional wooden houses within a community for risk or resilience assessment under cyclonic wind conditions.

1. Introduction

Tropical cyclones represent one of the most significant natural hazards for the population and the built environment of Madagascar, and traditional houses are particularly vulnerable to cyclonic winds. During cyclones, 10-minute sustained wind speeds at 10 m height over open water of more than 100 km/h (~28 m/s) are common in the coastal districts of Madagascar, which can last for several hours depending on the severity of the cyclone. This wind speed level corresponds to a severe tropical storm category based on the Southwest Indian Ocean scale.

Traditional houses in Madagascar represent more than 90% and 70% of houses in rural and urban areas, respectively. In highland regions, towards the centre of Madagascar, earth materials using fired or non-fired bricks [1] or unshuttered cob make up more than 90% of houses [2,3] (Fig. 1a). In contrast, more than 80% of traditional houses are made of wood and other plant-based materials in coastal districts (Fig. 1b). Traditional wooden houses in the coastal regions of Madagascar are particularly vulnerable to cyclones due to their locations and construction methods; thousands of wooden houses collapse or are severely damaged annually when a cyclone occurs. For instance, the

* Corresponding author.
E-mail addresses: rafik.taleb.dz@gmail.com, rtaleb@ed.ac.uk (R. Taleb), rilaidama@yahoo.co.uk (H. Ramanantoa), t.reynolds@ed.ac.uk (T. Reynolds), christopher.beckett@ed.ac.uk (C.T.S. Beckett), yuner.huang@ed.ac.uk (Y. Huang), mrakotoarivony@conservation.org (M. Rakotoarivony), a.gagnon@ljmu.ac.uk (A.S. Gagnon), landriamaro@conservation.org (L. Andriamaro).

https://doi.org/10.1016/j.engstruct.2023.116220
Received 2 October 2022; Received in revised form 17 April 2023; Accepted 23 April 2023
Available online 9 May 2023

Bureau National de Gestion des Risques et des Catastrophes (BNGRC; French for The National Office for Risk and Disaster Management) of Madagascar [4] reported that during each cyclone season between 2007 and 2012, 178,821 people were on average affected, among whom 56,795 were displaced, and causing damage to more than 50,000 houses, predominantly in coastal regions where cyclones make landfall. Hence, this study focuses on assessing the impact of cyclones on traditional wooden houses in two coastal study sites situated to the East of the country: Antalaha and Fénérive-Est, both historically known for their high exposure to cyclones (Fig. 2).

Residential buildings constructed with light wooden frames are especially vulnerable to extreme wind loadings. Although the effects of wind loading on the built environment have been studied previously [5,6], quantifying cyclonic wind-induced damages, especially for low-rise wood frame constructions, has only been recently studied by researchers in cyclone-prone regions [7–18]. These studies have mostly focused on the fragility of the roof components of engineered-type constructions and emphasised the importance of the strength of their connections on their performance. However, very few studies dealt with wind performance of non-engineered and heritage wooden constructions [19–21] and, to our knowledge, no fragility models are found in the literature for traditional wooden houses in Madagascar. This study focuses on the understanding of the structural performance of traditional wooden houses in the coastal regions of Madagascar under high wind loads. For this purpose, a set of in-situ and laboratory testing was carried out to evaluate the strength of the different components and connections according to the local construction practices of these traditional houses. A fragility analysis methodology was also used to evaluate the probability of failure of traditional houses under different wind loads to potentially increase our understanding of their performance under cyclonic winds.

2. Research methodology

Fig. 3 presents a general overview of the research methodology used in this study. The study begins with a review of construction practices and guidelines for traditional wooden houses and the assessment and classification of cyclone-induced damages. Two coastal study sites were selected to understand the construction practices, specifically, the connection types used for structural and non-structural members, and to plan an experimental program for field testing to assess the strength of different types of members and connections. The wind speeds for calculation of forces imposed on the structure refer to the 10-minute sustained wind speed measured at 10 m height in open terrain, as appropriate for use with the Eurocode wind probabilistic model [24]. Based on this model and the test results, the fragility curves were then developed using a Monte Carlo simulation technique by considering the two orthogonal directions of the houses for wind loading. Details about each aspect of the cyclone-damage assessment, field testing, and fragility analysis are provided in the following sections.

3. House typologies and construction practices

3.1. Traditional wooden houses in coastal regions

Traditional wooden houses in the coastal regions of Madagascar typically comprise a one-room family dwelling in a rectangular layout generally varying between an area of 10 m^2 and 30 m^2. Depending on traditional practices and the locally available materials (wood, plants, and earth), different house typologies are found across the various coastal regions of the country. However, the *Falafa*, as illustrated in Fig. 1b, are the most common wooden house type along the east coast. Construction methods for *Falafa* houses include embedded wooden columns into the ground that form the foundation system, with spacing ranging approximately between 50 cm and 150 cm, and which are connected at the top to tie beams that support the roof structure. The most popular configuration for the roof structure is a two-sided gable roof using a king post truss with a ridge beam and purlins. The roof structure is usually covered by dried palm leaves while traveller's palm panels are often used as cladding walls. Roof cover and wall claddings are usually roped or nailed to the structural members.

Structural members for columns, beams and roof truss are usually made of unsawn wood poles of approximately 5–15 cm in diameter or rough-cut 5–15 cm square sections and are jointed using pegged or nailed mortise-tenon (MT) joints. The floor is typically elevated from the ground level and usually not connected to the columns; hence, it is independent from the structural system.

The wood species and shape used for *Falafa* houses depend on cost and local availability. Although prepared materials are sold in urban centres, people in rural areas may collect them in nearby areas at no charge. Getting the material for building houses has nonetheless become more difficult recently because of increased deforestation in the East of Madagascar. Other housing types, especially in urban areas, may include corrugated metal sheets for roof cover, unreinforced cement block with metal sheet roofs, and a combination of wood and raffia with metal sheet roofs. Structures comprising fired masonry or concrete are highly desirable but are outside the price range for most of the population living in the coastal regions.

Fig. 4 and Fig. 5 show the typical components and layout of typical traditional wooden houses and their roof structure, respectively, in the coastal regions of eastern Madagascar. These non-engineered structures are typically built with very little or no technical engineering input and are often the product of varied construction traditions and cultures.

3.2. Construction guidelines for traditional wooden houses

Guidelines [25] to improve the construction techniques of traditional wooden houses were launched in 2016 by the *Cellule de Prévention et Gestion des Urgences* (CGPU; French for Emergency Prevention and Management Unit), a public agency for disaster management. The guidelines suggest some techniques to improve the resistance of traditional houses to cyclonic winds, considering the different traditional house typologies found across the coastal regions of Madagascar and the technical capacities and materials available to local communities. These

Fig. 1. Typical (a) earthen houses in highlands and (b) wooden houses in coastal regions of Madagascar.

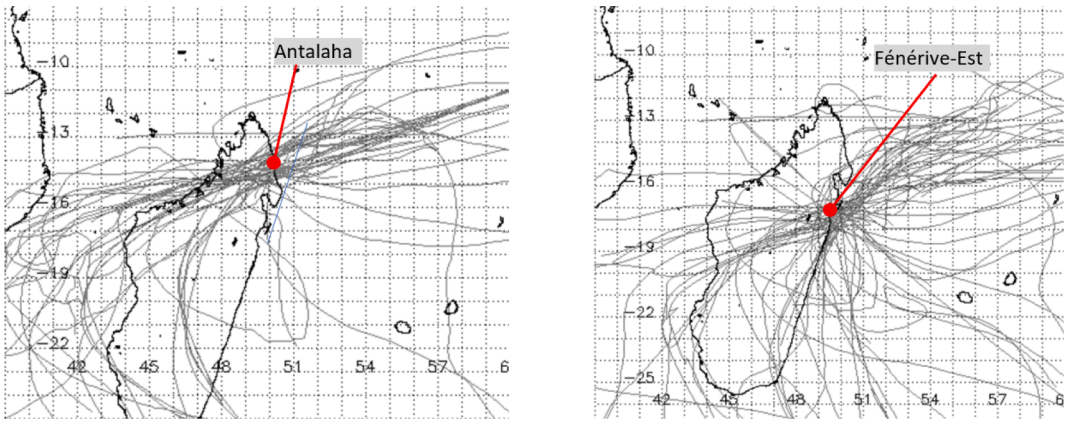

Fig. 2. Cyclones that have passed through the 1-degree resolution grid cell covering the cities of Antalaha (left) and Fénérive-Est (right) since 1880. The cyclone tracks used to produce these figures were obtained from the International Best Track Archive for Climate Stewardship (IBTrACS) project [22,23].

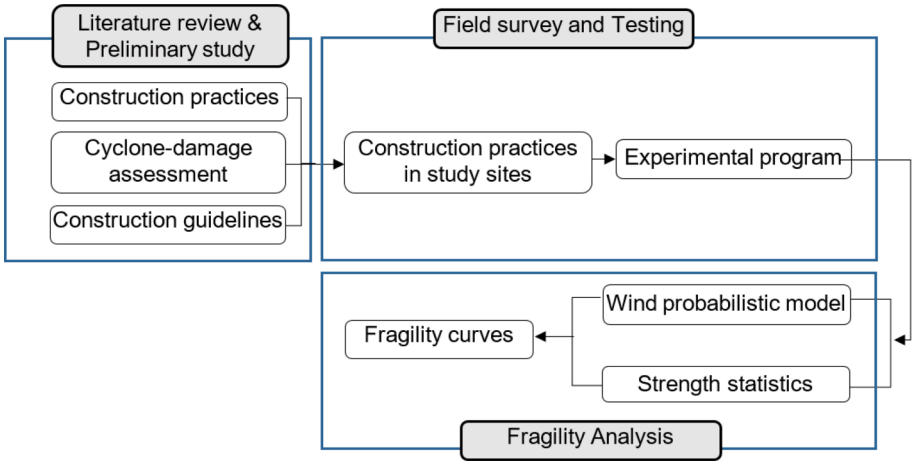

Fig. 3. Research methodology.

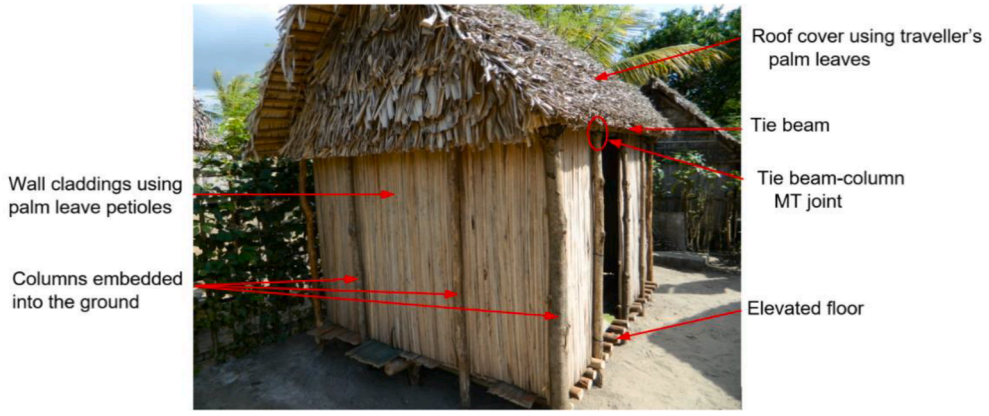

Fig. 4. Component of a typical wooden house in the coastal regions of eastern Madagascar.

guidelines were intended to be used by local people to build their houses without requiring highly skilled workmanship.

These construction guidelines were developed following field surveys at six locations based on diagnosis of house typologies, actual construction techniques, and the analysis of the effects of cyclones on houses. The guidelines show, through graphical illustrations for different traditional house typologies, some general principles for choosing construction sites, tools and materials to use, and the different construction steps to follow from earthwork and land preparation to roof cover and wall cladding. Fig. 6, for instance, illustrates the different steps to follow for constructing a *Falafa* house that start by embedding the corner columns. The guidelines, however, neither recommend specific sizes for structural members nor do refer to technical engineering parameters for measuring the strength of members and connections, although they provide some general rules on how to make MT joints to connect the different structural members. The guidelines further mention that there is a research gap on the resistance of Malagasy wood species and connections used in construction.

Fig. 5. Roof components of a typical wooden house in the eastern coastal regions of Madagascar.

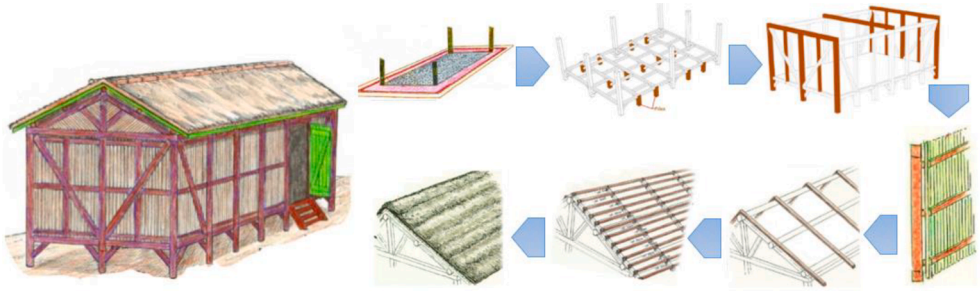

Fig. 6. Construction steps for a *Falafa* type traditional wooden house. Adapted from [25].

The guidelines recommend using galvanised annealed steel wire to join roof secondary members and purlins. The guidelines also highlight the importance of lateral bracing and a minimum embedment depth of the wooden columns down to 75 cm in general and to 100 cm for sandy soils. They state that a shallow column's embedment of 50 cm might be ineffective in resisting strong wind loads and lead to house collapse by overturning the whole structural system.

3.3. Survey of wooden houses in the study sites

Surveys of traditional houses in the two coastal sites of Antalaha and Fénérive-Est were carried out in 2018 by the research team. The surveys showed that the *Falafa* house typology is the dominant type at the two locations. The structural system and the different house components at the two sites are as described earlier in this section. A substantial number of houses were, and still are, self-built based on enduring local construction practices and using low or no-cost materials collected from nearby areas or forests. It was noticed that many of these traditional wooden either do not have windows or have a unique small window on only one side.

Wrapped or nailed connections are usually used to join the roof cover to secondary members and secondary members to purlins, while MT joints are used to connect the structural members of roof truss system to the tie beams and then to the columns. The roof truss is usually composed of a king post truss at each end of the house, supporting the top ridge beam, and two mid-purlins connected to the rafters. Depending on the length of the house, an additional truss may be included at mid span of the long tie beams. It was observed during the surveys that use of the mid-purlins was omitted in many cases, and the secondary members were supported only at their ends by the ridge beam and the tie beams.

The wrapping materials used for connections are usually plant-based. Plastic-based wraps are occasionally used, which are obtained by cutting the plastic mesh used in mosquito nets or for agricultural purposes. The plant-based wraps identified in the study sites were Sisal, traveller's palm leaves, and *Zavy*. *Zavy* is a local name for the outer bark of a local tree species that is soft enough to be used as a rope for wrapped connections.

MT connections are nailed or pegged using a single nail or dowel. However, different geometrical configurations for the mortises and the tenons are commonly used, and those seen in the study sites were rectangular, circular, or conical (Fig. 7). MT joints of inferior quality, notably with a loose tenon that is not well fitting into the mortise, were commonly seen. These different connection configurations were considered in the subsequent experimental and field-testing campaigns to assess their strengths.

The surveys showed that shallow column embedment depths of 50 cm or even less is common practice in the construction process with column spacing ranging generally between 50 cm and 150 cm. Moreover, the absence of lateral bracing was found to be common practice as well.

4. Cyclone-induced damage for traditional wooden houses

4.1. Types of cyclone damage

To estimate the extent and severity of the damage caused by cyclones that made landfall in Madagascar in the past 40 years, we collected and analysed data from BNGRC-Madagascar. After each cyclone, the damage report tabulates the number of affected people and the extent of the damage to houses and infrastructure in the affected regions and districts. The recording of damage data started with cyclone *Kamisy* in 1984. Fig. 8 represents the number of damaged wooden traditional houses for cyclone seasons from 2012/2013 to 2019/2020 where available data on affected traditional houses categorize the damage into either total collapse or partial damage. Partial damage refers to the removal of the roof cover or cladding walls without or with minor damage to the structural system. Most of the cyclone during this period have made landfall or threaten the east and north coastal regions.

The 2016/2017 cyclone season was particularly devastating due to cyclone *Enawo* that made landfall in March 2017 along the coast of Sava (North-east Madagascar) between the cities of Sambava and Antalaha. The cyclone generated sustained wind speeds of 210–230 km/h (~58-

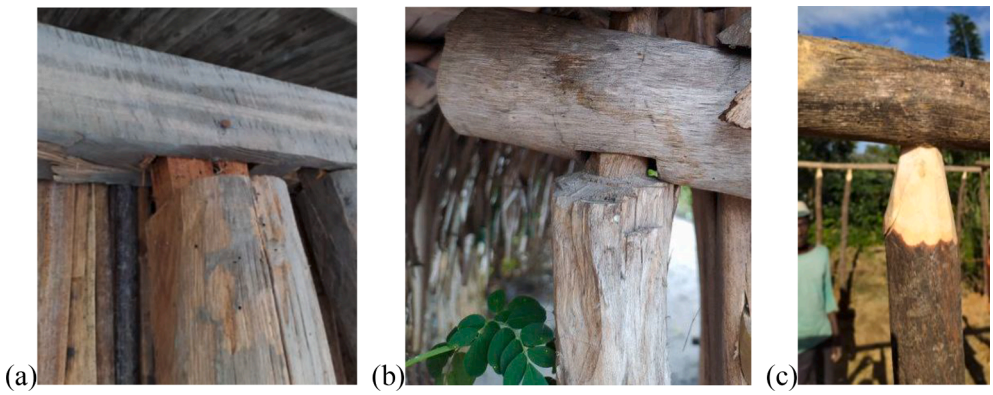

Fig. 7. Identified types of MT joints in the study sites: (a) rectangular tenon; (b) circular tenon; (c) and conical tenon.

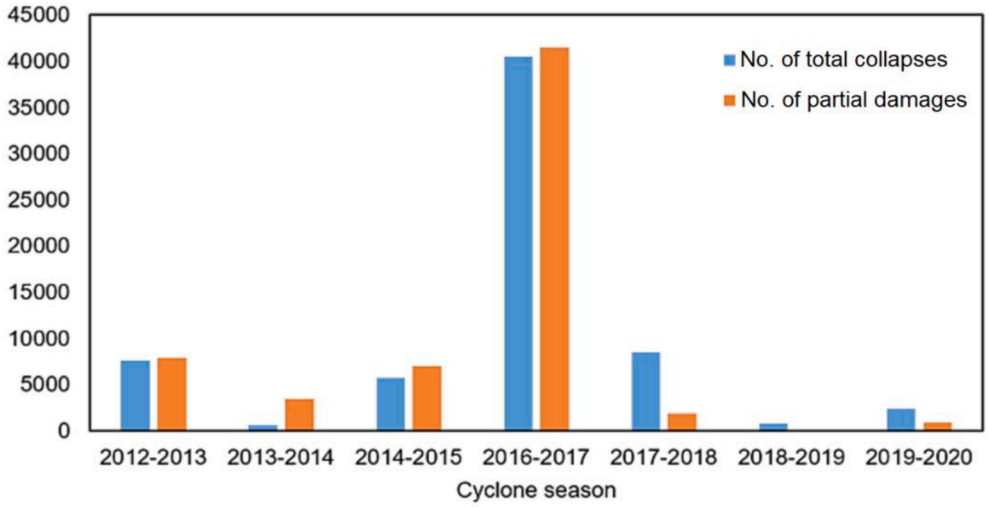

Fig. 8. Number of affected traditional wooden houses per cyclone season.

64 m/s), corresponding to a very intense tropical cyclone category based on the South-West Indian Ocean scale [26,27]. Antalaha was the most affected city during the passage of this cyclone, with about 30% of its traditional housing stock affected.

4.2. Assessment of cyclone-induced damage

Knowledge from damage assessment is an important step in the evaluation, repair and reconstruction, of the built environment, as well as for future planning and design. However, the data collected or made available for damage assessment are generally imprecise, and engineering judgement is needed to assess structural damage. Furthermore, previous studies on the assessment of wind damage on wood-frame structures [28–30] were mostly associated with engineered structures or structures that are constructed to prescriptive standards based on industry experience in the related country. The traditional wooden houses in Madagascar are non-engineered construction that are usually self-build according to local practices that may differ from region to region. This makes assessing their cyclone-induced damage a difficult process [31,32].

Ralijoana [32] reported that construction guidelines applicable to buildings built in the so-called “high- cyclonic zones”, as published by the Ministry of Public Works of Madagascar in 1988, highlight the significant types of damage caused by cyclones, which were identified based on the analysis of the damage engendered by cyclones *Kamisy* (1984) and *Honorinina* (1986). *Kamisy* was at the time considered the worst cyclone to strike Madagascar since 1911. Different types of damage were reported and listed according to their frequencies. Amongst those damages, the roofing sheet cover and its connections were identified as the most vulnerable since about 80% of the cyclone-related damage was observed to have affected the roofs of structures, of which more than 50% were related to the fixity of the roof sheets. The fastening system of the sheets to the roof elements was estimated to represent 35% of damages. However, it is not clear if this type of damage reflects that of recent cyclones that have struck Madagascar during the last two decades as no other and more recent study on assessing damage to traditional wooden houses could be found.

Securing photographic evidence in the aftermath of a cyclone is also rare and difficult to plan. Therefore, photographic evidence of damaged traditional wooden houses was sought from online media sources following some cyclonic events that struck Madagascar between 2004 and 2022. Photos for a total of 24 damaged traditional wooden houses were collected and by examining those photos for observed wind-induced damage, it was possible to identify the main recurrent damage patterns. It is emphasized, that due to the reduced number of assessed houses, results showed in Fig. 9 represent only a qualitative nomination of the weakest links in these traditional wooden houses where damage is likely to produce under cyclonic wind.

In general, the types of damage may be categorized into either secondary damage related to roofing cover and wall cladding removal without compromising the structural system or structural damage leading to the failure of structural members or their connections. Nine distinct types of damage were identified and listed according to their frequencies, as shown in Fig. 9. From these observations, it was found

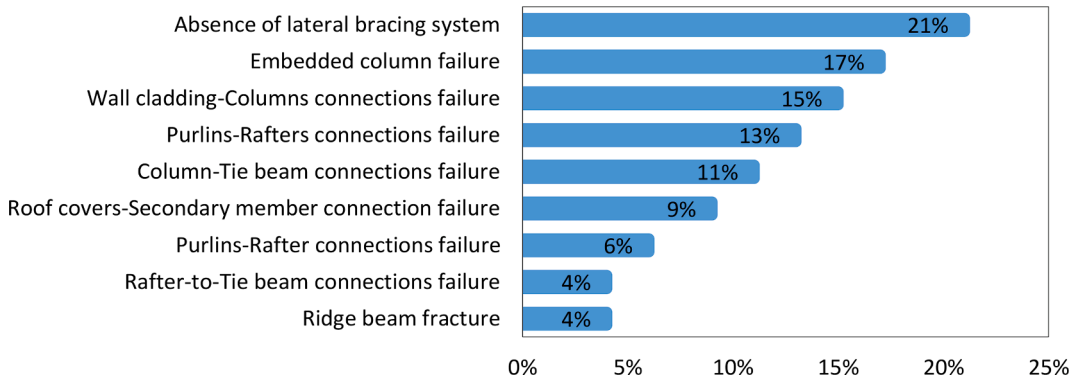

Fig. 9. Damage evaluation based on photo interpretation of selected traditional houses following cyclones during the period 2004–2022.

that approximately 50% of damage due to cyclones is related to the roof system, similarly to previous findings by Ralijoana [32]. Among the types of damage related to the roof system, weak connections between secondary members and purlins were the most influential causing 18% of this type of damage. Fracture of columns' bases or failure due to weak column embedment into the ground was also a type of failure leading to extensive damage to the vertical structural system.

4.3. Factors influencing the damage on the roof and wall cladding

Fig. 10 shows several houses with distinct levels of damage to the roof structural system and wall cladding. The structural roof system is usually a king post truss with a ridge beam and two purlins supported at mid-span of the rafters. Secondary members that hold the roof cover are placed perpendicular to the purlins with a spacing of approximately 50 cm and connected to them by either nailed or wrapped connections. Roof cover-secondary member and secondary member-purlin connections may be qualified as a secondary type of damage (Fig. 10a, Fig. 10b), whereas purlin-rafter and rafter-tie beam connections may be recognized as primary damage to the roof system (Fig. 10c, Fig. 10d). Wall cladding is connected to the columns using wrapped connections and related damage is also categorised as secondary damage (Fig. 10d, Fig. 10b).

4.4. Factors influencing vertical system failure

The collected photographs show that structural damage is, in many cases, associated with an extensive leaning of the structural system (Fig. 11), which is due to either the inclination of the embedded columns, because of insufficient soil reaction, or fracture at the column base. Fracture of columns at their base may be attributed to the strength of the wooden column but, more importantly, to the degree of rot at the base of the columns, resulting in reduced strength or even loss of ground connection and structural integrity.

These types of damage usually lead to an extensive damage situation due to the large inclination of the structural system or even its total failure. These types of structural damages would also be associated in many cases with the absence of diagonal bracing in the frame that provide lateral stiffness. Surveys in the study sites confirmed that, although required by the construction guidelines for traditional wooden houses, construction without lateral bracing system is a widespread practice.

5. Experimental programme

5.1. Experimental methods

A testing program was set to evaluate the strength and failure modes

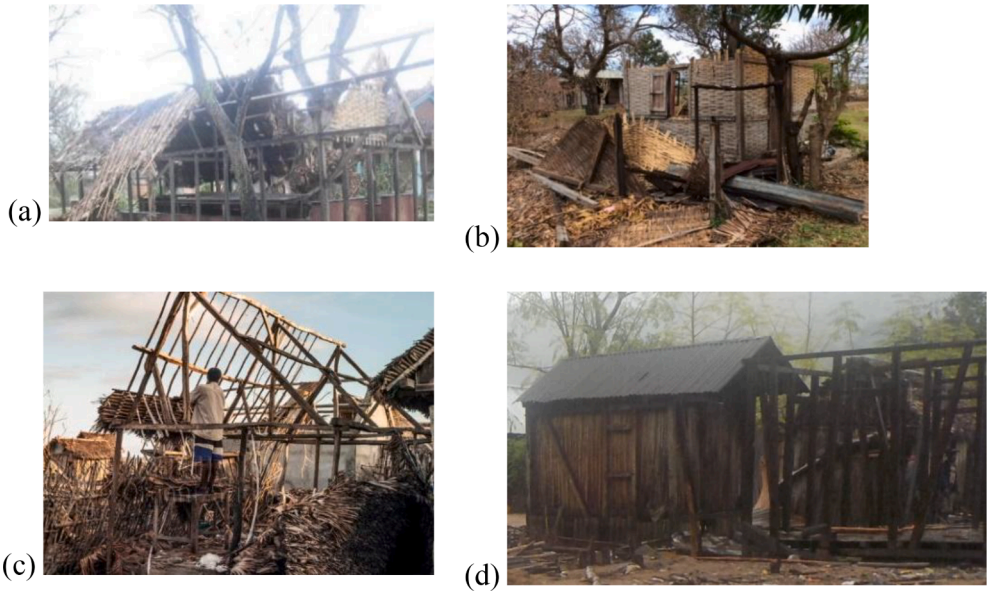

Fig. 10. Different damage types observed in Falafa roof systems and wall cladding. (Copyright (a) & (b) Macolline Madagascar, (c) WHO Photo Library, (d) R. Ntsiva N. Andriatsitohaina).

Fig. 11. Traditional wood houses with total failure of the structural system. (Copyright AIC-Madagascar).

of the different members and connections of traditional wooden houses, noting that no available data exists in the literature or in the CPGU guidelines that characterise their strengths. A portable testing rig, illustrated in Fig. 12, was designed and built to test the different connection configurations that have been identified as widely used in the coastal site-study regions. The testing rig was used to test wrapped connections, Mortise-Tenon joints under axial and lateral forces and a 3-point bending test for wooden members. The load was applied using a 45 kN capacity cylinder with a manual hydraulic pump and measured using a 50 kN compact load cell. The rig was sufficiently light, collapsible, and robust to be deployed to remote locations by a crew of two researchers in a suitable vehicle.

The test specimens for connections were made from wood collected locally and built by local craftsman according to their own practice and knowledge. The tests were conducted in the site study regions to reflect similar moisture content conditions for wood species and soils as for the wooden houses and to increase community interest. Each connection configuration was replicated in 8 to 10 specimens and tested to measure their strengths and its variabilities. Other tests included wood compression test, bending test of wood members, embedded wooden columns under lateral load, and soil characterisation and are presented in the following sections.

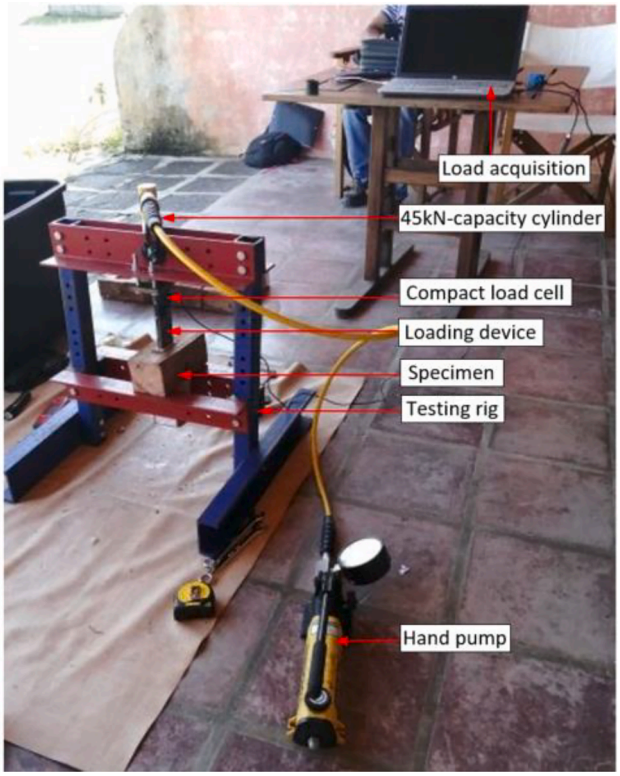

Fig. 12. Portable testing rig.

5.2. Tests programme and specimens

5.2.1. Testing of member–member wrapped connections

Different purlin-secondary member connection configurations were considered for testing to estimate their strength. Test specimens were made by local builders in the three considered study regions to reflect local construction practices. The specimens comprised 200 mm long sections of the wood member used for purlins and secondary members, connected at the mid-points. Seven different types of connections were considered based on field observation of constructions practices: single nailed connection, wrapped connections using Sisal, wrapped connection using traveller palm leaves, wrapped connection with *Zavy* rope, wrapped connection with mosquito net, single nailed with wrapped connection with *Zavy* rope, and single nailed with wrapped connection using mosquito net. For nailed connections, nails with 4.5 mm diameter and 70 mm length were used; these are typical nails available to use by local builders. Different wrapped connections were tested using traveller's palm and *Zavy* as plant-based ropes, and mosquito net as plastic-based rope. A combination of nailed with *Zavy* or mosquito net rope were also considered assuming that these combinations may contribute to assuring more strength to this type of connection.

For each type of connection, a series of 10 specimens were tested. Fig. 13 shows these different tested connections. The load was applied to the specimen using a steel device made by bolted steel (Fig. 13a). The secondary member part of the connection was placed on the two parallel steel supports, and the parallel two heads of the U-shape device were placed between the purlin and the loading cylinder. The load was gradually increased until failure. The three types of wrapping materials that were identified as being widely used for traditional house construction were tested to evaluate their strengths: *Zavy*; traveller's palm leaves; and mosquito net. The experimental setup to test roof cover connections was similar to that of wooden members wrapped connections with 10 specimens tested for each type of connection. Acacia wood species was used for the specimens.

5.2.2. Testing of Mortise-Tenon connections

The mortise-tenon joint (MT joint) is the most common joint used in traditional Malagasy wooden houses. This type of joint is used to connect columns to tie beams as well as the roof truss system to the columns. Building surveys showed different configurations of how local builders construct those mortise-tenon joints depending on the shape of the tenon. The performance of traditional MT joints has been previously evaluated experimentally [33–35]. However, traditional MT joints used for traditional wooden houses present some differences regarding their shapes and methods of construction. Three geometries were identified and tested: rectangular; circular; and conical (Fig. 14). The common way for local carpenters to make these connections is by using hand tools, resulting in a non-perfect fit between the mortise and the tenon parts. Wooden pegs or nails are then used to connect the two parts. A series of

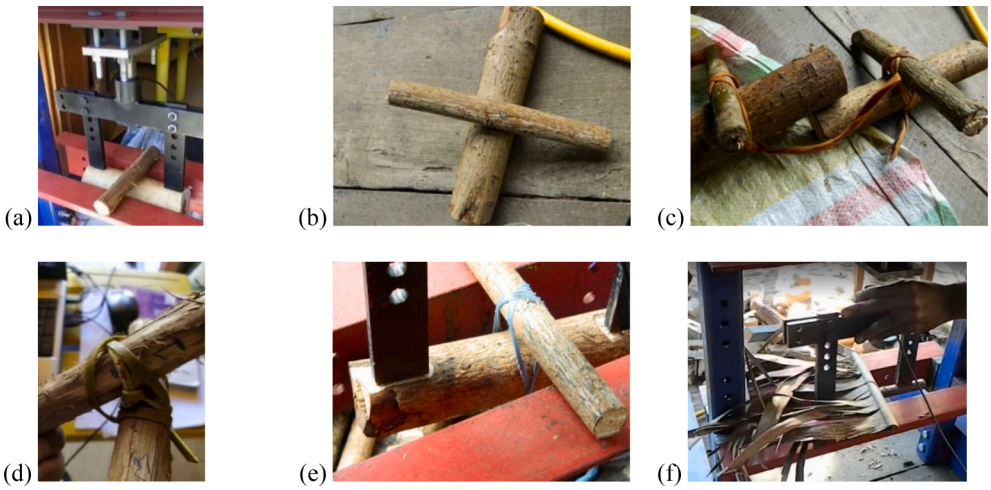

Fig. 13. Purlin-secondary member connections (a) specimen test setup, jointed by (b) nail, (c) Zavy (d) Traveller's palm leaves, and (e) Mosquito-net ropes, and (f) secondary member-roof cover (palm leaf petiole) connections test setup.

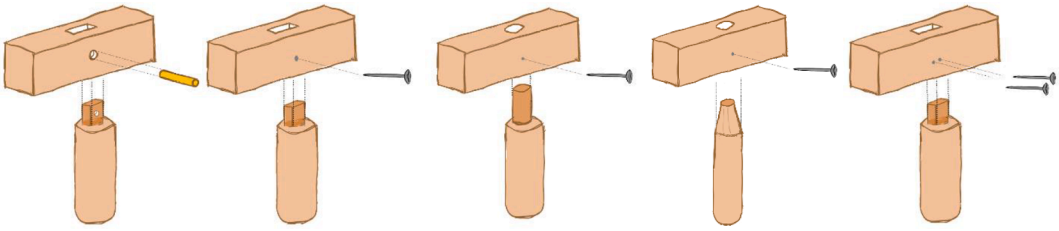

Fig. 14. Mortise-Tenon test specimen configurations (a) MT-PRec (b) MT-NRec (c) MT-NCir (d) MT-NCon (e) MT-DNRec.

mortise-tenon joints with different configurations were constructed by local builders in the two coastal study regions and tested under direct and bending moment to measure pull-out strength and bending strength, respectively. The test specimens were constructed with 10 replications for each configuration. Eucalyptus wood was used for MT joint specimens tested in Fénérive-Est, while mortises and tenons components were made using wood species locally known as *Canelle* and *Rahiny*, respectively. These wood species are locally widely used for the construction of these traditional wooden houses and were later characterised by measuring their density, moisture content and compressive strengths (see Section 5.2.3).

The tested specimen configurations were pegged MT joint with rectangular tenon (PRec), and nailed MT joint with rectangular tenon (NRec), circular tenon (NCir) and conical tenon (NCon) (Fig. 14). For rectangular shape MT joint, the joints were constructed by using a tenon tongue with a cross section of about 30 mm × 80 mm and a depth of 50 mm. MT joint with circular tenon were made by using a mortise hole diameter of 55 mm with an embedment of 50 mm for the tenon tongue. A wooden peg with 18 mm diameter and nails with 4.5 mm diameter and 90 mm long where used. The double nailed rectangular (DNRec) MT joint, although not practiced (as mentioned above), was considered for comparison purposes to the other configuration and to explore whether such a configuration could strengthen the connection when considering cyclone effects on those traditional wooden houses. Tests with two nails were not considered: although two nails would seem a natural extension of local practices (and trivial to a Western perspective on construction), the cost to the builder of additional nails is unrealistic.

For mortise-tenon joints tested under axial load, the mortise hole crossed all the member depth in order to expose the top of the tenon to the loading jack. This allowed a compressive axial load to be applied to the head of the tenon, rather than requiring a direct pull-out tension force (thus avoiding issues surrounding anchoring of the tensile grips and crushing of the tenon). Fig. 15a shows the experimental setup for axially tested MT joints. The mortise member part was placed as shown in Fig. 15 and the loading device applies load as a compression force on top of the tenon.

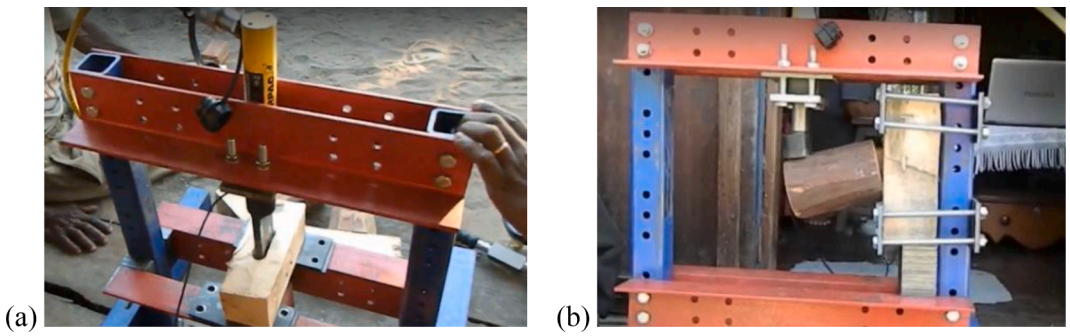

Fig. 15. Experimental setup for (a) pushout test and (b) bending test of MT joints.

Fig. 15b shows the experimental setup for a bending test of the MT joint with a rectangular configuration. The mortise member part was mounted to one of the steel stands of the loading frame (right- side of the frame in Fig. 15b) and fixed in place by bolted steel plates. The load was vertically applied at the free end of the tenon members at a distance of 200 mm to the inner face of the stand of the test rig.

5.2.3. Compression and flexural tests of wood

Wood specimens collected from different wood species used for Malagasy wooden houses in Antalaha and Fénérive-Est were cut into cubes of 50 mm dimension for compressive strength evaluation parallel and perpendicular to the grain. Three cube specimens were considered for each test configuration. Due to the load limitation of the test rig used for connections testing, compression tests were conducted at the National Laboratory of Public Works and Building in Madagascar using a universal testing machine. The moisture content and density (adjusted to 12% moisture content) of the cube specimens were measured before each compressive test. Table 1 gives the different measurement and test results.

Eucalyptus and Acacia wood from Fénérive-Est were tested in three-point bending using roughly sawn beam specimens (Fig. 16). The bending test was carried out using the test rig with a distance between the points of support of 500 mm with load applied at mid-span. The Modulus of Rupture (MOR) was calculated as:

$$MOR = 3F_{\max}a/(bd)^2 \quad (1)$$

with F_{max} is the maximum applied load, a is mid-span distance, b and d are the width and depth of cross-section, respectively. Six beam specimens were tested for each wood species. The MOR's mean and standard deviation were 64.3 MPa and 5.3 MPa, respectively, for Eucalyptus wood, and 38.4 MPa and 1.13 MPa for the Acacia wood.

5.2.4. Lateral load testing of embedded wooden columns

A series of static tests on the laterally loaded embedded columns were conducted to determine the effects of embedment depth and soil conditions on lateral capacity. A total of 12 tests were performed, six in each of the two study regions in Fénérive-Est and Antalaha. However, tests in Fénérive-Est were not conclusive as a load capacity could not be reached due to the winch's wire distance limit and therefore are not reported herein. The test comprised a pull winch with a capacity of 40 kN, anchored to a sturdy tree, which was used to apply lateral load to the column. Displacement was measured from a reference vertical post or interpreted from video documentation.

The tests for the six embedded columns (all Eucalyptus, diameter approximately 110 mm) in Antalaha were conducted in a sandy soil for embedment depths of 50 cm, 75 cm, and 100 cm, with two tests for each depth. The 50 cm embedment depth correspond to the common practice in the study sites and most coastal regions according to local builders. While, according to CPGU Guidelines [25], 75 cm is the recommended depth with 100 cm recommended for sandy soils. The embedded columns were placed in the soil in an approximately 20 cm diameter hole and the soil was manually tamped around the column in several lifts,

Fig. 16. Setup for the 3-points flexural test for wooden beams.

which reflects the local construction practice. The test setup comprised a radial configuration (6 m radius) around an existing tree used as a reaction column (Fig. 17a). The lateral force was applied at a height of 0.5 m from the ground surface using a manual pull winch mounted between two cargo slings that were attached to the embedded column at one end and to the existing tree at the other (Fig. 17b and Fig. 17c). The applied load was measured by a load cell of 20 kN capacity attached between the sling and winch wire.

5.3. Tests results and discussion

5.3.1. Wrapped connections

The different observed failure modes are shown in Fig. 18. Table 2 and Fig. 19 give the mean and standard deviation of the load capacity of each type of specimens. All single-nailed specimens failed due to pull out of the nail from either the purlin or the secondary member, while wrapped connections failed due to tension failure of the wrapping material. Those three types of connection showed the lowest strength. On the other hand, failure of *Zavy* and mosquito net wrapped connections showed two different failure modes due to either the tension failure of the wrapping material or the failure of the secondary member at mid span. For roof cover-secondary member connections, all specimens failed was due to the failure of the petioles. The mean and standard deviation for the strength were found to be 0.22 kN and 0.09 kN, respectively.

Notably, nailed connections were shown during field survey as being widely used as mean of purlin-secondary member connections, despite

Table 1
Wood properties tested in compression.

Wood species	Local name	Location	Moisture Content (%)	Density (kg/m^3)	Strength (MPa)	
					// grain	⊥ grain
Symphonia fasciculata (Hazinina)*	Aziny	Antalaha	14	953.7	61.26	11.66
Manilkara laciniata Lecomte	Nanto		13	938.9	65.59	34.36
Eucalyptus (species unknown)	Eucalyptus		14	947.5	58.44	18.66
(Genus and species unknown)	Canelle		12	663.2	47.83	13.94
Capurodendron ludiifolium Aubrév	Rahiny		9	1236.2	69.87	47.36
Acacia (species unknown)	Acacia	Fénérive-Est	30	546.2	20.91	4.57
Eucalyptus (species unknown)	Eucalyptus		35	506.6	25.52	20.56

* Vulnerable IUCN Red list.

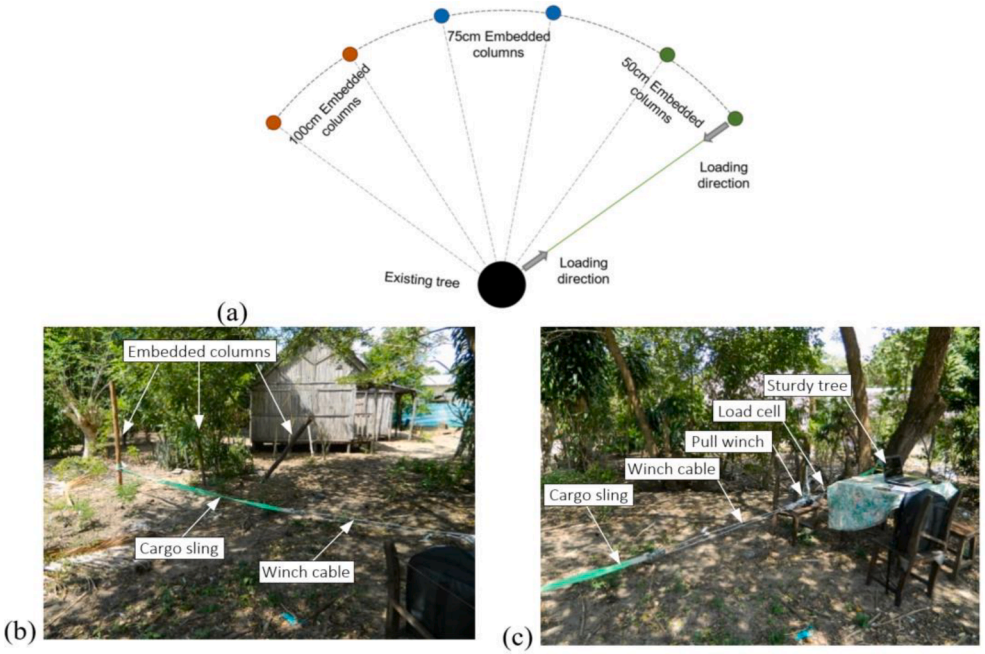

Fig. 17. Test setup for embedded column under lateral load (a) setup layout and (b) sling connection to an embedded column and (c) to an existing tree.

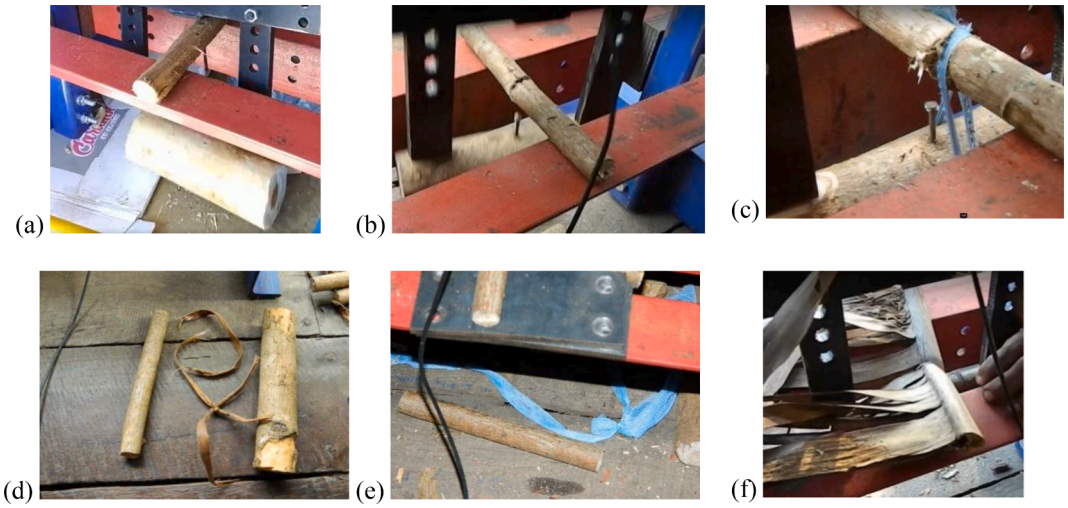

Fig. 18. Observed failure modes for (a-e) member–member connections failed by rupture of wrapping materials, and for (f) for secondary member-roof-cover connections with petiole failure.

revealing the second weakest performance of the testing connection types. Traveller's palm was found to be the weakest among the tested types of connection. On the other hand, *Zavy* and mosquito net wrapped connections showed higher strength. The combination of nailed and wrapped connections using *Zavy* and mosquito net ropes demonstrated the highest strength among all test types of connections, suggesting the benefit of using these wrapping materials as a way of strengthening connections.

5.3.2. *Mortise-Tenon joints*

Two types of failure modes were observed for axially loaded MT joints. The first category of failure was due to grain tension splitting of the mortise, observed for pegged MT joints. The second was observed for single nailed MT joints and was due to the splitting failure of the tenon member driven by the bending deformation of the nails. For double nailed MT joints, both failure modes due to splitting of the mortise member and the tenon were observed (Fig. 20). Table 3 and Fig. 21 gives the mean and the standard deviation of the load capacity for each connection configuration.

Table 4 and Fig. 22 gives the mean and the standard deviation of the load capacity for each test configuration. Three categories of failure mode were observed for laterally loaded MT joints. The first was due to grain tension splitting of the mortise member (observed for pegged MT joints, which were similar to failures observed for axially loaded pegged MT joints), and the second was due to the splitting failure of the tenon at the contact line with the nail, driven by the bending deformation of the nails (Fig. 23). The third category of failure mode was observed for double nailed MT joints and was due to the tension splitting of the tenon.

5.3.3. *Testing of embedded wooden columns*

The response curves for moment versus rotation is shown in Fig. 24a. The moments and rotations were evaluated around a centre of rotation at two third of the embedment depth based on Bowling simplified model [36]. It is notable that lateral strength is significantly reduced by

Table 2
Load capacity (mean and standard deviation) of the wrapped connection test specimens.

Specimen ID	Specimen description	Test location	Load capacity (kN)	
			Mean	S.D. (COV)
W-TPalm	Wrapped connection using traveller palm leaves	Fénérive-Est	0.76	0.36 (0.48)
W-Nail	Nailed connection	Antalaha Fénérive-Est	1.19	0.35 (0.29)
W-Zavy	Wrapped connection using *Zavy* rope	Antalaha	1.45	0.54 (0.37)
W-MNet	Wrapped connection using Mosquito-net rope		1.56	0.59 (0.38)
W-NZavy	Nailed + *Zavy* wrapped connection		1.76	0.70 (0.40)
W-NMNet	Nailed + Mosquito-net wrapped connection		2.00	0.54 (0.27)

Note: For each type of connection, 10 replicated specimens were tested to estimate the mean and COV, except for W-TPalm, where only 3 specimens were tested.

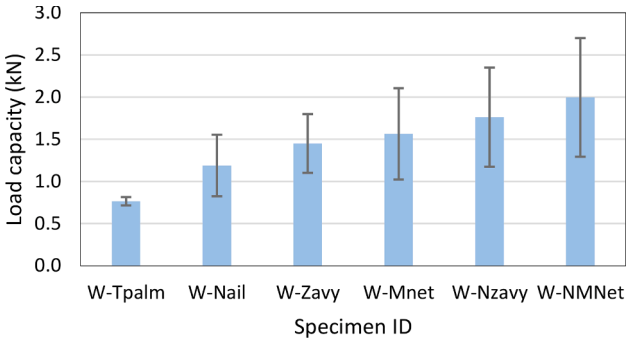

Fig. 19. Load capacity (mean and standard deviation) of the wrapped connection test specimens.

reducing the embedment depth of the columns. By reference to 50 cm embedment depth as the common construction practice for wooden traditional houses, increasing the embedment to 75 cm and 100 cm increase the lateral capacity by 3 times and 6 times, respectively. The lateral capacity versus embedment depth for each test are plotted in Fig. 24b.

6. Fragility analysis

Fragility is defined as a conditional probability of exceeding a specific limit state as a function of an intensity measure (wind speed herein). The probability of component failure, p_f, is defined as:

$$p_f = Pr[G(X) \leqslant 0] = Pr[R - W \leqslant 0] \quad (2)$$

where $G(X)$ is the limit state function defined as resistance minus load, and X is the vector of random variables representing a resistance or a loading random variable acting on the system. $G(X) \leq 0$ denotes failure or a defined limit state exceedance. For this study, R represents the resistance and W is the wind load. Resistance and wind load are modelled probabilistically due to their variability and uncertainty. It should be noted that the dead load for these houses is mainly related to the self-weight of the components and although it may play a beneficial role, it was not accounted for since the dead load for such light-frame houses is relatively small compared to wind load and may be conservatively neglected.

In this study, the wind fragility curves are developed using a Monte Carlo simulation approach. This approach generates realizations for thousands of permutations of the random demand and capacity variables from their specified distributions and evaluates whether wind-induced failure occurs by using the limit state function $G(x)$. The procedure is repeated for a range of wind speeds to complete the fragility curve. The capacity distributions are based on the experimental testing discussed above. The design wind loads were derived based on the Eurocode 1 model [24,37]. The fragility function of the structural component system is commonly modelled using the lognormal cumulative distribution function and the fragility model is given by

$$F(x) = \Phi[(\ln(x) - \lambda_R)/\xi_R] \quad (3)$$

where $\Phi[.]$ denotes the standard normal cumulative distribution

Table 3
Load capacity statistics for axially loaded mortise-tenon test specimens.

Specimen ID	Specimen description	Test location	Number of samples	Load capacity (kN)	
				Mean	S.D. (COV)
MT-PRec1	MT joint - Pegged with Rectangular tenon	Fénérive-Est	10	7.07	1.84 (0.26)
MT-NRec1	MT joint - Nailed with Rectangular tenon		8	4.31	1.39 (0.32)
MT-NCir	MT joint - Nailed with Circular tenon		10	3.23	0.84 (0.26)
MT-NCon	MT joint - Nailed with Conical tenon		10	3.84	0.93 (0.24)
MT-PRec2	MT joint - Pegged with Rectangular tenon	Antalaha	9	6.87	0.96 (0.14)
MT-NRec2	MT joint - Nailed with Rectangular tenon		10	6.35	1.44 (0.23)
MT-DNRec	MT joint - Double Nailed with Rectangular tenon		9	9.31	2.29 (0.25)

(a) (b) (c) (d)

Fig. 20. MT joints failure modes under axial load for (a) pegged (b) nailed and (c, d) Double nailed with rectangular tenon specimens.

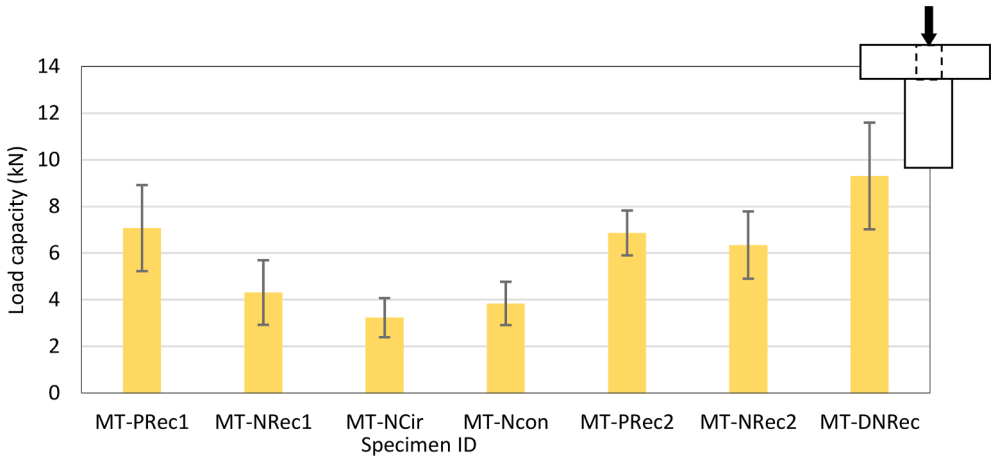

Fig. 21. Load capacity of Mortise-Tenon joints for tested specimens under axial load.

Table 4
Load capacity (mean and standard deviation) of the laterally tested mortise-tenon specimens.

Specimen ID	Specimen description	Test location	Load capacity (kN)	
			Mean	S.D. (COV)
MT-PRec1	Pegged MT joint with rectangular tenon	Fénérive-Est	7.82	2.98 (0.38)
MT-NRec1	Nailed MT joint with rectangular tenon		5.35	1.63 (0.31)
MT-NCir	Nailed MT joint with circular tenon		5.79	1.90 (0.33)
MT-NCon	Nailed MT joint with conical tenon		7.88	2.78 (0.35)
MT-PRec2	Pegged MT joint with rectangular tenon	Antalaha	7.94	2.01 (0.25)
MT-NRec2	Nailed MT joint with rectangular tenon		8.08	1.48 (0.18)
MT-DNRec	Double nailed MT joint with rectangular tenon		6.01	2.02 (0.34)

Note: For each type of connection, 10 replicated specimens were tested to estimate the mean and COV.

function, x is the intensity measure (the 10-minutes wind gust speed herein), λ_R and ξ_R are, respectively, the logarithmic median and standard deviation of the resistance R.

Fragility assessment was performed for a baseline traditional wooden house type typical in coastal regions of Madagascar considering various construction practices for connections that have been experimentally assessed. The failures are defined for different damages states and are related to the strength of various components of the structure being exceeded. Thus, fragility curves are first developed for each of the components experimentally tested, then the damage to particular components is assigned to a damage state, and finally those results are combined to give a fragility curve for the baseline house. Some variations to the baseline house are investigated to show their effect on its fragility curve.

6.1. Description of the baseline house

The house geometry adopted for this study is based on surveys at the study sites visited in Fénérive-Est and Antalaha. The structural frame consists of a one-story house with a gable roof. The house has a plan dimension of 4 m by 6 m and a height of 2.5 m from the ground to the peripheral beam with roof slope of 40°. The elevated floor is not considered to affect the wind path since the common practice for it is to be constructed independently of the structural system.

6.2. Wind load model and statistics

The primary factors which influence wind loading on structures are the free-field wind velocity, the effect of the local environment (usually referred as roughness effect), and the interface between the wind and the structure (represented by a pressure coefficient). The Eurocode wind

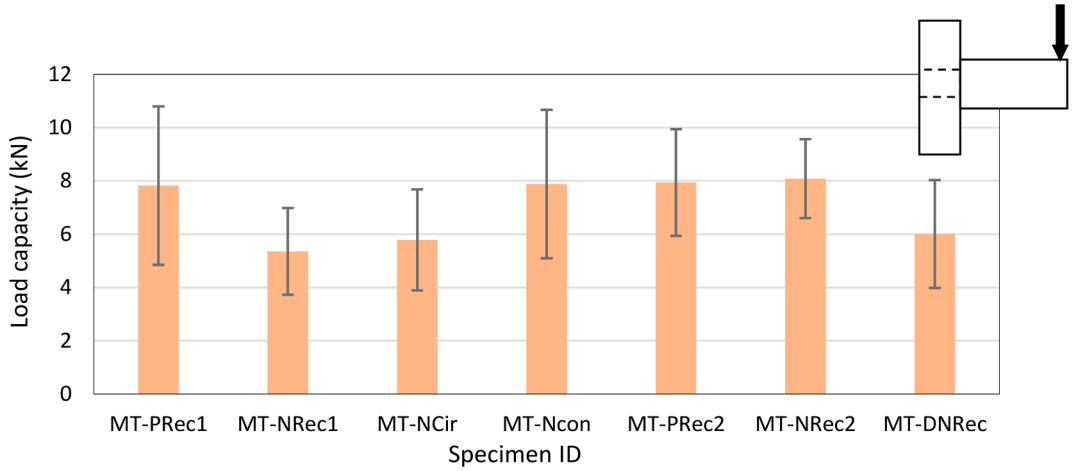

Fig. 22. Load capacity of Mortise-Tenon joints for tested specimens under lateral load.

(a) (b) (c) (d)

Fig. 23. Mortise-Tenon joints failure modes under lateral load for (a) pegged (b, c) nailed and (d) double nailed with rectangular tenon specimens.

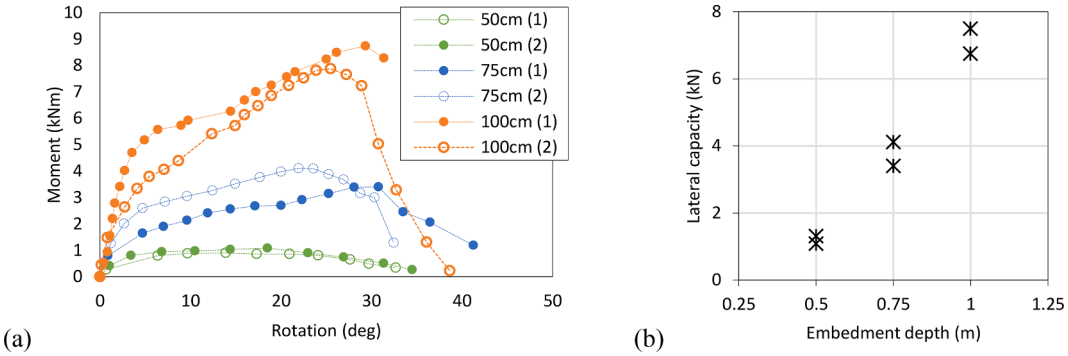

Fig. 24. Embedded column lateral test response (a) load–displacement response curves and (b) lateral capacities for the different considered embedment depths.

probabilistic model was used in this study to calculate the wind load [37,38] based on a refinement of the JCSS model [24]. The Eurocode probabilistic wind hazard demand model is established using the 10-minute mean wind speed at a height of 10 m above flat open-country terrain as the wind hazard intensity measure, and this wind speed is used in the wind load calculation procedure. However, the peak gust wind speed, usually averaged over two seconds, is required to obtain the effective peak static load distribution as used for structural design. Therefore, a gust factor, which is the ratio of the expected peak wind speed to the average wind speed, is used to convert the mean wind speed to the peak gust wind speed. According to the Eurocode, the wind action on a structural component is given by:

$$q_w = c_r \times c_g \times m_q \times q_{ref} \tag{4}$$

in which c_r is the roughness factor, c_g is the gust factor for velocity pressure, m_q is the model uncertainty factor, and q_{ref} is the reference free-field wind velocity pressure given by:

$$q_{ref} = 0.5 \times \rho_a \times c_p \times V^2 \tag{5}$$

With ρ_a is the air density 1.225 kg/m^3, c_p is the pressure coefficient, and V is the basic wind velocity defined as the 10-minute mean wind velocity at 10 m height above a flat open terrain. Table 5 summarises the wind load statistics, based on the JCSS model [16], used in this study. As shown in Fig. 25 and Table 6, the wind pressure coefficients are adjusted for each partitioned zone based on the Eurocode 1 methodology. The wind-force resisting system is considered as an assemblage of connection types and structural members that work together to provide support and stability for the overall structural system. Roof cover and wall cladding are defined as elements of the house envelope that transfer the load to the main wind-force resisting system. Roof cover is assumed to transfer wind load to the secondary members and purlins before being transferred to the roof truss system and tie beams, while wall claddings transfer the wind load directly to the columns. Each member can be assumed to perform as individual components being loaded directly by the wind, with its equivalent tributary area for a critical location of a roof cover or the wall cladding.

Table 5
Wind load statistics.

Parameter	Description	Mean	COV	Distribution
c_r	Roughness factor	0.80	0.10	Normal
c_g	Gust factor	1.00	0.10	Normal
c_p	Pressure coefficient	See Table 6		
m_q	Model uncertainty factor	0.80	0.20	Normal

6.3. Resistance statistics and damage states

The strengths of the different members and connections are used as the engineering demand parameter corresponding to a specific failure or damage state. Strength statistics related to the different types of connections are based on the test results presented earlier (Section 4) follow a normal distribution and are given in Table 7. Negative values for resistance generated in the Monte-Carlo simulation were treated as zero. It is not considered unreasonable, given the wide variation in the measured strengths, that a very small number of components may have critical flaws which leave them with essentially zero load capacity. It may be that the people erecting the building would recognise these very weak joints during construction and apply some strengthening or repairs, but such an effect is beyond the scope of the present study. Nonetheless, assuming the normal distribution is censored at zero strength is not physically meaningful. This will result in a small overestimate of the probabilities of failure presented here for some components, less than 1% for most cases but not more than 3%. Strengths for wall cladding-column connections were assumed to be half of the corresponding strengths of the tested member–member wrapped connections as tests were conducted using two-wraps whilst one-wrap is the common practice to connect wall cladding to columns.

Due to the limited number of tests for the embedded wooden columns under lateral load, deterministic values for lateral strength were taken. Based on a simplified bilinear curve fitting of the average moment-rotation curves for each of the three-embedment depth considered in the tests (Fig. 26), three damage states were defined for three levels of column rotation. Damage state 1 (DS1) corresponding to column rotation of 5° that indicates slight damage, and damage state 3 (DS3) corresponding to 25° column rotation for 75 cm and 100 cm

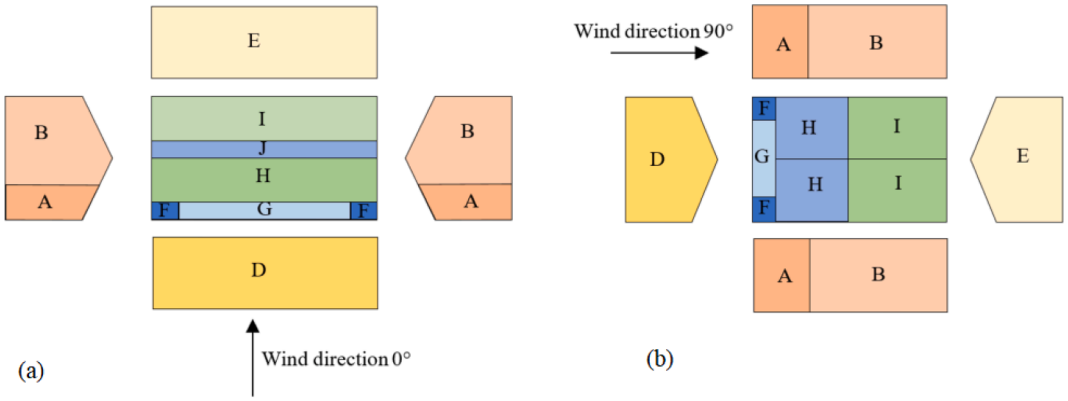

Fig. 25. Repartition of wind pressure zones on the structure according to Eurocode 1 model for (a) wind direction (0°) and (b) wind direction (90°).

Table 6
Statistics for external pressure coefficients.

Partitioned zone	Mean		COV
	Wind direction 0°	Wind direction 90°	
A	−1.27	−1.19	0.10
B	−0.97	−1.08	
D	0.99	0.95	
E	−0.51	−0.40	
F	0.70	−1.50	
G		−2.00	
H	0.60	−1.18	
I	−0.20	−0.50	
J	−0.30	/	

Table 7
Statistics for connections strength.

Component	Connection type	Mean (kN)	SD (kN)	Distribution
Roof cover-secondary member connection	Petiole	0.22	0.09	Normal
Secondary member-purlin connection	W-TPalm	0.76	0.36	
	W-Nail	1.19	0.35	
Purlin-rafter connection	W-Zavy	1.45	0.54	
	W-MNet	1.56	0.59	
Wall cladding-column connection	M−net	0.78	0.30	
	Zavy	0.73	0.27	
	TP leaves	0.38	0.18	
Rafter-tie beam connection	MT-PRec	7.07	1.84	
Tie beam-column connection	MT-NRec	4.31	1.39	
	MT-NCir	3.23	0.84	
	MT-NCon	3.84	0.93	

embedment depths and 20° for 50 cm embedment depth. DS2 was defined as the intermediate situation between DS1 and DS3. DS1 and DS3 correspond, respectively, to a yield damage state where the soil around the column remains essentially elastic and ultimate damage state corresponding to the ultimate capacity where no further extra load could be sustained by the column under a lateral load.

For the building-level fragilities, three damage states were separately defined for the roof system and the vertical system. A limited damage state (DS1), intermediate damage state (DS2), and extensive damage state (DS3) relate to different damage indicators as shown in Table 8. Each damage state is defined as the occurrence of any of the corresponding damage indicators and in either orthogonal wind directions. For the roof system, DS1 was related to damage of secondary member-purlin connections, DS2 and DS3 to 50% and 100% loss, respectively, of the connections in the roof system. The vertical system damage states were related to the damage of either wall claddings or columns. Damage of columns was attributed to either the embedded columns' inclinations, as defined previously and presented in Fig. 26, or the fracture of columns at their bases. Fragility due to the fracture of wooden columns was considered assuming sound wood with a circular cross-section of 100 mm diameter, and the MOR of Eucalyptus wood tested in Fénérive-Est (Table 1). Reduction of geometrical and mechanical properties due to rotted wooden columns are not considered in this study.

6.4. Component-Level fragility curves

6.4.1. Roof component failures

Fig. 27 shows fragility curves for the different components constituting the roof system for the trigger of damage corresponding to the most loaded roof zone. The curves are presented for roof cover-secondary members, secondary members-purlins, and purlins-rafter connections. For each type of these connections, fragilities were assessed for the weakest and the strongest strengths, that is traveller's palm leaves and mosquito net wrapped connections for secondary members-purlins connections, nailed and mosquito net wrapped connections for purlin-rafter connections, pegged rectangular MT joint and nailed circular MT joint for rafter-tie beam connections.

As had been observed during the field survey, the use of the mid-purlin or roof truss at mid span of the tie beams were omitted in several cases; these presence of absence of the mid-purlin was therefore also considered when evaluating the fragility curves. Fig. 27a and b show the case of roof system with and without mid-purlin, respectively. It is shown in both cases that the purlin-rafter connections are the weakest links in the roof system that may lead to roof damage.

The median wind speeds for purlin connections' damage are equal to 28 and 26 m/s for the two considered types of connection using nail and mosquito net rope. That these wind speeds are so similar, despite the range of strengths considered, clearly indicates that the purlin-rafter connection types considered have little influence on their probabilities of failure and the roof damage is likely to be driven by damage of the purlin connections. The median wind speeds for the two secondary member-purlin connection types considered are equal to 60 and 42 m/s for traveller's palm leave and mosquito net wrapped connections, respectively, for the case without mid-purlin. For the case of a roof with a mid-purlin, the median wind speeds corresponding to traveller's palm connections is 59 m/s while it exceeded the considered wind speed limit of 80 m/s for mosquito net wrapped connections.

The presence of a mid-purlin has a considerable effect in reducing failure probability of secondary member-purlin connections due to the reduction in the corresponding tributary area. As shown in the figure, the presence or not of the mid-purlin may change the damage trigger from the secondary member-purlin connections to the rafter-tie beam connections. This later may lead a complete failure of the roof system as the example of the house shown on the right in Fig. 10.

Fragilities related to the roof structure damage trigger with different

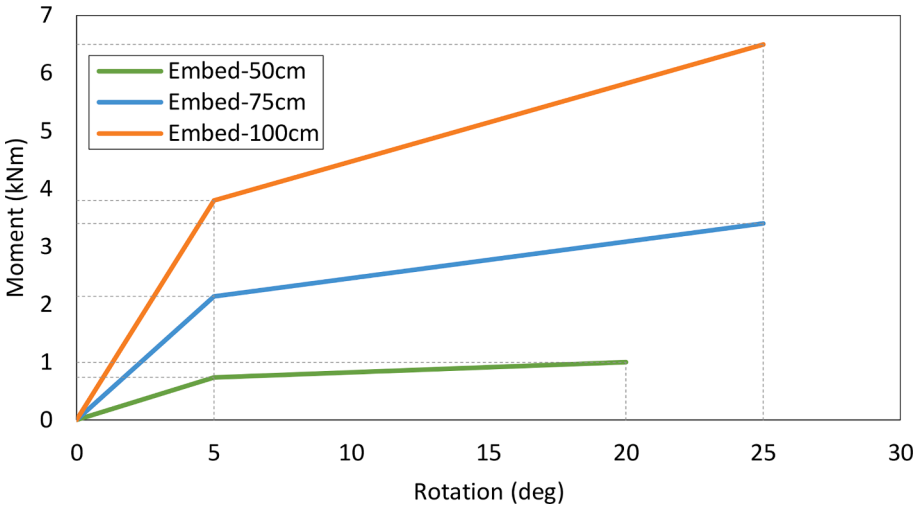

Fig. 26. Bilinear response model for average moment-rotation response curves.

Table 8
Definition of damage states.

Damage state	Damage indicators					
	Roof system			Vertical system		
	Secondary member-purlin connections	Purlin-rafter connections	Rafter-Tie beam connections	Wall claddings	Embedded columns inclination	Columns fracture
DS1	< 15%	NA	NA	< 25%	< 5°	NA
DS2	< 50%	< 50%	< 50%	> 80%	< 15°	NA
DS3	NA	~ 100%	~ 100%	NA	> 25°	Yes

Note: NA- Not Applicable.

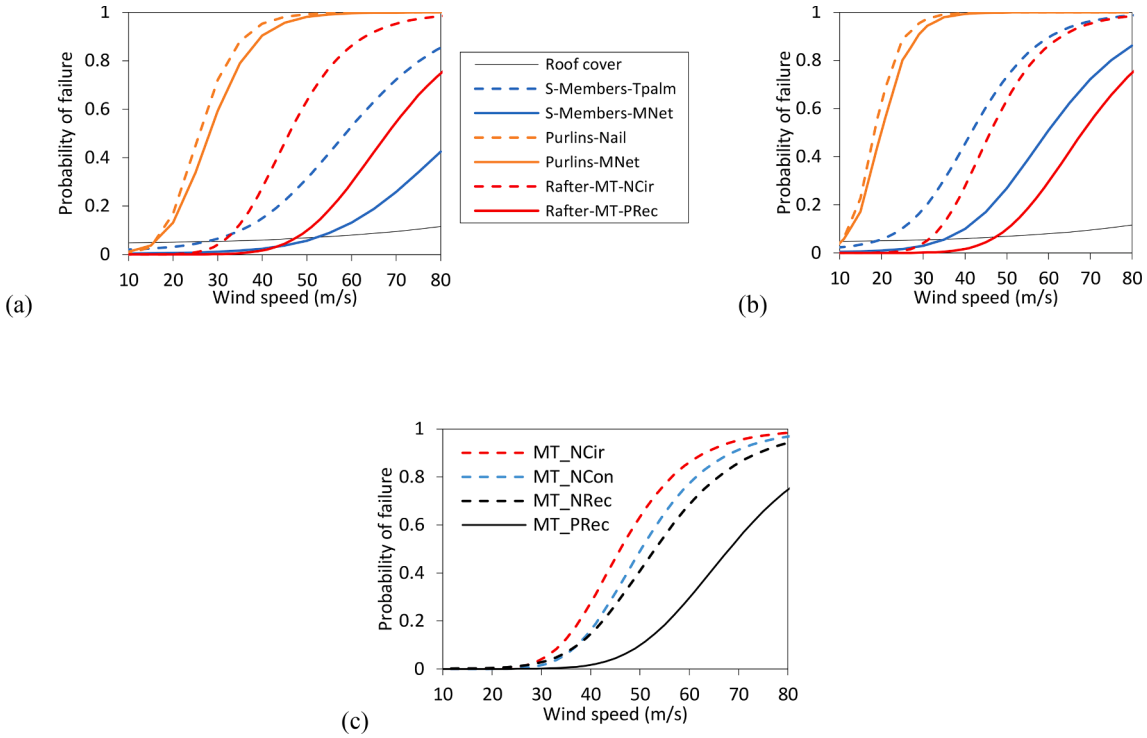

Fig. 27. Fragility curves for (a) roof members wrapped connections for roof with mid-purlin, (b) roof members wrapped connections for roof without mid-purlin, and (c) Rafter-Tie beam MT connections.

rafter-tie beam MT joint types are shown in Fig. 27c. The median wind speeds for nailed circular, conical, rectangular, and pegged rectangular are 46, 50, 53, and 68 m/s, respectively. This clearly shows the advantage of pegged MT joint in resisting uplift of the roof structural system compared to the other considered MT joint types. The strength of the roof cover to secondary member connections means it is unlikely that damage appears at connections between these two members prior to other connections in the roof system.

6.4.2. Wall cladding failure

Fig. 28 shows fragility curves for wall cladding for three connection schemes to the columns using Traveller's palm leaves and mosquito net wrapped connections for the cases of columns spaced by 0.5 m and 1.5 m. These three connection schemes are schematically represented in Fig. 28c and considers the number of connections points of the wall cladding along the height of the columns. The strength of the Traveller's palm leaf wrapped connections is approximately half the strength of the mosquito net wrapped connection. For each of the wall cladding connection schemes, the median wind speeds for the case with Traveller's palm leaves wrapping materials is about 65–70% higher than the case using mosquito net. On the other hand, reducing column spacing from 1.5 m to 0.5 m, increases the median wind speeds required for damage by approximately 60%.

6.4.3. Embedded columns failure

Fig. 29 shows fragility curves for column embedment of 50 cm, 75 cm, and 100 cm, considering columns spacing of 0.5 m, 0.75 m, and 1.0 m. For each combination of column embedment depth and spacing, fragility curves are drawn for yield (DS1) and ultimate (DS3) limit states, and for column fracture.

For example, in the case of 1.0 m column spacing, increasing column embedment depth from 50 cm to 75 cm would increase median wind speed for DS3 from 29 m/s to 53 m/s, and to 74 m/s for 100 cm embedment depth. The results of the fragility analysis indicate that increasing the column embedment from 50 cm to 75 cm increases the median wind speed to cause damage by approximately 45%, and increasing the embedment from 50 cm to 100 cm would increase the median wind speed by approximately 60%.

While the use of 50 cm column embedment has shown limited performance, reducing column embedment from 100 cm to 75 cm would need a reduction of the column spacing to have a comparable resistance. For the wood properties considered, the likelihood of column fracture at the base is always less than the likelihood of soil failure due to large column rotation. As mentioned previously, a foundation system using wooden columns embedded to 50 cm was found to be widespread practice for traditional houses in eastern coast regions in Madagascar and that would be the main reason for complete structural system failure for traditional wooden houses without lateral bracing (the presence of rot notwithstanding).

6.5. Building-level fragility curves

6.5.1. Roof system fragility

Fig. 30 presents roof system fragility curves for the case mosquito net for wrapped connections, and by considering two cases of MT joints for rafter-tie beam connections: nailed MT joints with circular tenon; and pegged MT joints with a rectangular tenon. These represent the strongest and the weakest strengths for MT joints. As shown in Table 8, each damage state is defined as the occurrence of any of the shaded damage indicators in the corresponding row. It is noted that since all components do not necessarily participate in the definition of each damage state, the fragility curves may cross over one other. Purlin-rafter and rafter-tie beam connection failures do not contribute to the definition of DS1. Therefore, as shown in Fig. 30a, the fragility curve for DS1 is crossed by fragility curves for DS3. DS2 fragility curves present a higher probability due to using a unique mid-purlin in the roof system. For roof the structure using nailed MT joints with circular tenon for rafter-tie beam connections, the median wind speeds to exceed DS2 is 32 m/s but are identical for DS1 and DS3, equal to 61 m/s. Using pegged MT joints with rectangular tenon, the median wind speed exceeding DS3 is 70 m/s.

6.5.2. Vertical structural system failure

The vertical structural system fragilities were evaluated for different combinations of wall claddings connection schemes, spacing between columns, and column embedment depths into the ground for the three defined limit states. Fig. 31 and Fig. 32 show fragility curves for the case of 75 cm columns embedment depth considering mosquito net wall-column connections considering loosely (scheme 3) and tightly wall-column connections (scheme 1) as defined in Fig. 28c. Fig. 33 and Fig. 34 show similar fragility curve for the case of 100 cm columns embedment depth. As shown in Table 8, DS3 limit state is related only the ultimate rotation of the embedded columns. It is shown that for the case of 50 cm column embedment depth, fragilities for all limit states are related to the column rotations at the base with not much difference between three limit states, as a slight increase in wind speed of about 5 m/s is sufficient to induce the limit state corresponding to extensive damage of the structural system. On the other hand, and for the cases of 75 cm and 100 cm column embedment depths, DS1 and DS2 are related to wall-column connections. In these cases, it is shown that using tight wall-column connections shifts the fragility curves to the right and increases the median wind speed by approximately 20–25%. Overall, it was shown that fragilities for these traditional wooden houses and using the different traditional connection types presented in this study could be significantly reduced by reducing spacing between connection points and increasing column embedment depth to at least 75 cm.

7. Conclusions

This study investigated the performance of non-engineered traditional wooden houses in two coastal sites in eastern Madagascar under

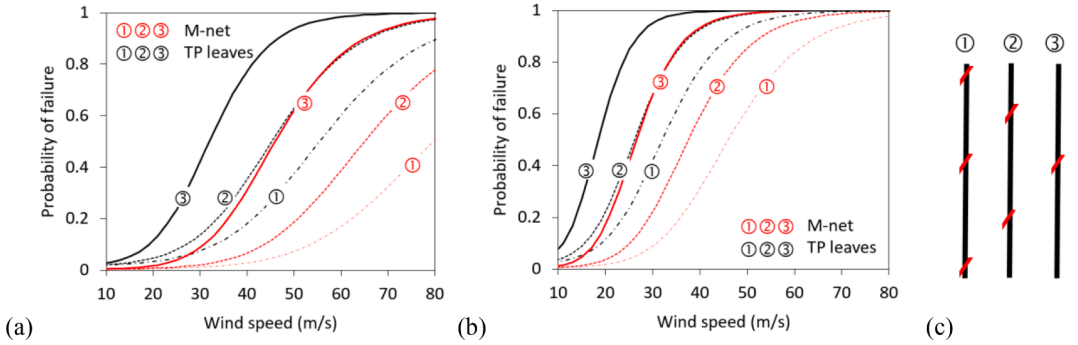

Fig. 28. Fragility curves for the cases of (a) 0.5 m columns spacing and (b) 1.5 m columns spacing (c) for the three wall cladding connection schemes to the columns.

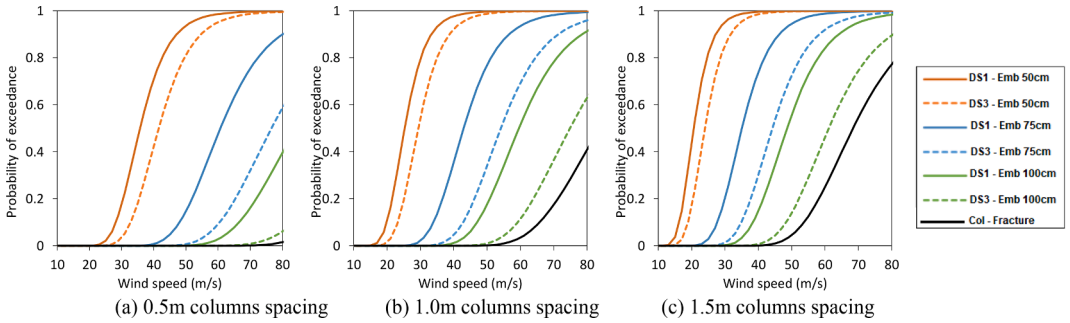

Fig. 29. Fragility curves for DS1 (yield), DS3 (ultimate), and column fracture limit states for embedded columns.

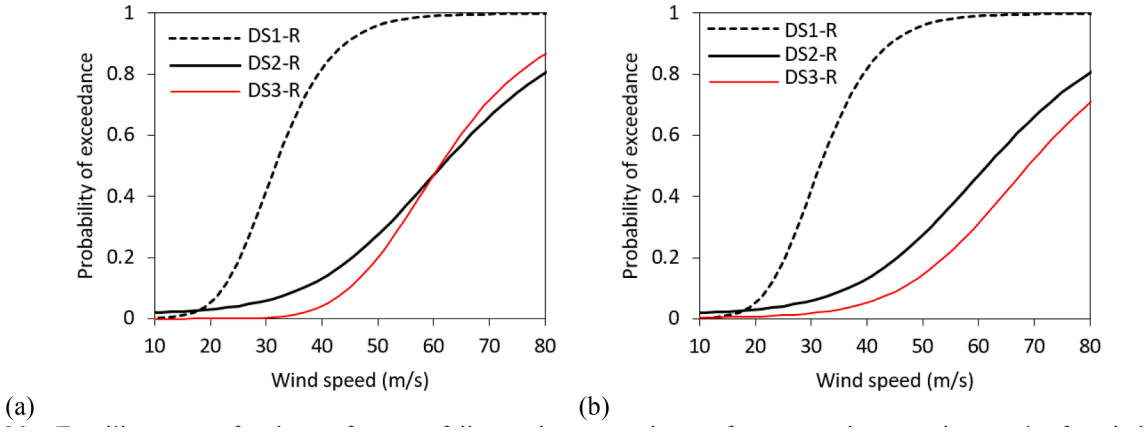

Fig. 30. Fragility curves for the roof system failure using mosquito net for wrapped connections and rafter-tie beam joint using (a) pegged MT joints with rectangular tenon, and (b) nailed MT joints with rectangular tenon.

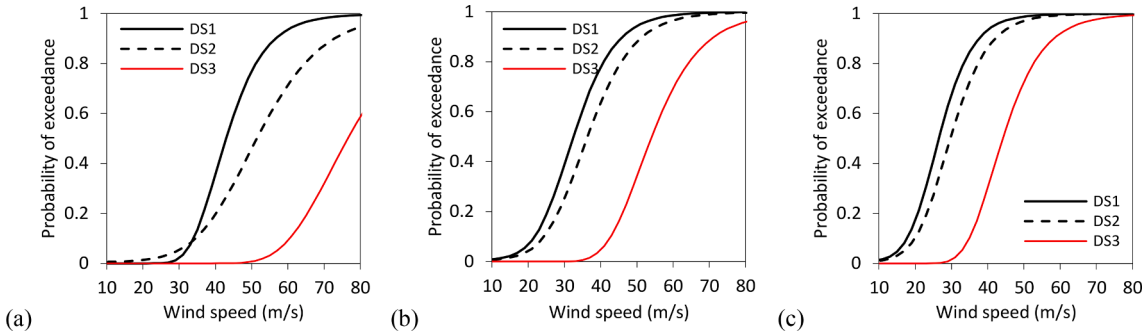

Fig. 31. Fragility curves for vertical members considering 75 cm column embedment and M−Net loosely wall-column connections: (a) 50 cm columns spacing, (b) 75 cm columns spacing, and (c) 100 cm columns spacing.

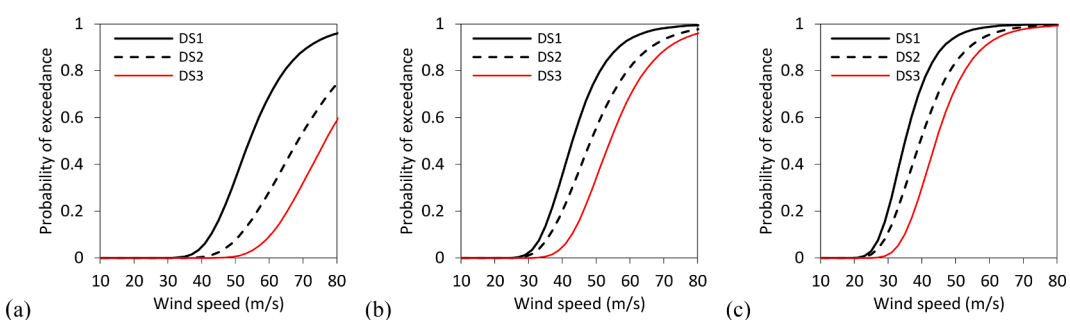

Fig. 32. Fragility curves for vertical system considering 75 cm column embedment and M−Net tightly wall-column connections: (a) 50 cm columns spacing, (b) 75 cm columns spacing, and (c) 100 cm columns spacing.

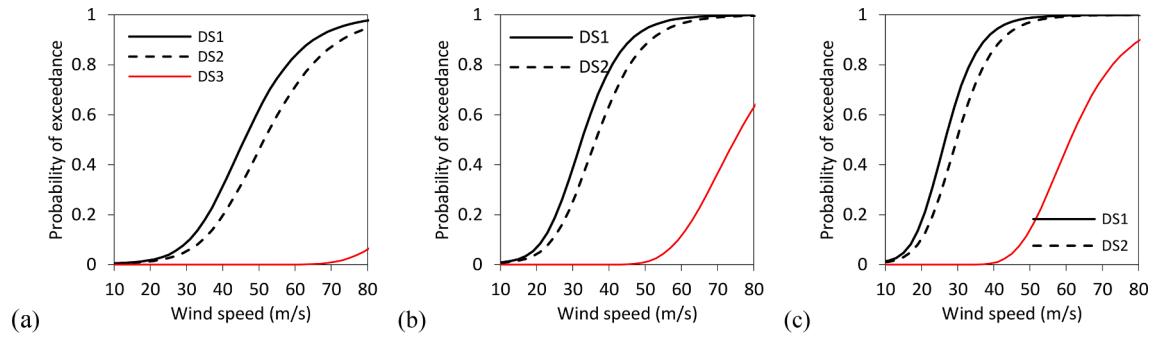

Fig. 33. Fragility curves for vertical members considering 100 cm column embedment and M−Net loosely wall-column connections: (a) 50 cm columns spacing, (b) 75 cm columns spacing, and (c) 100 cm columns spacing.

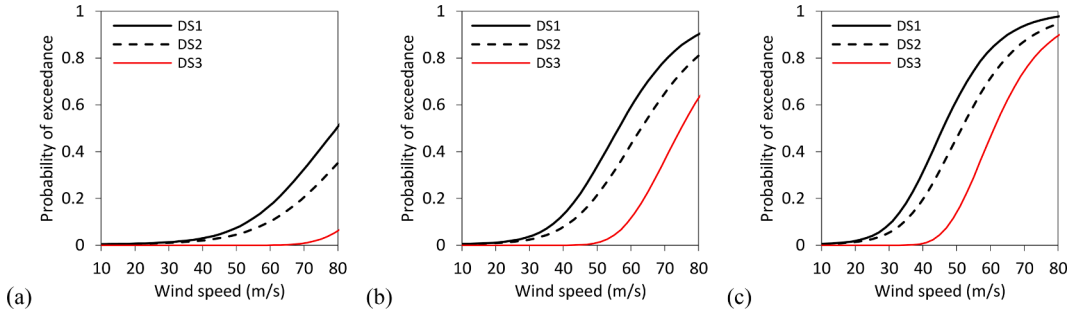

Fig. 34. Fragility curves for vertical system considering 100 cm column embedment and M−Net tightly wall-column connections: (a) 50 cm columns spacing, (b) 75 cm columns spacing, and (c) 100 cm columns spacing.

extreme wind loads. Assessments of cyclone-induced damage have shown that building failures are usually attributed to the collapse of the connections between members and the columns embedded into the ground. Field surveys in Antalaha and Fénérive-Est have revealed that wrapped connections and artisanal mortise-tenon joints are the two types of connections used to connect wooden members for these constructions. Different types of ropes used for wrapped connections and other shapes of mortise-tenon joints made with locally available materials and tools, and the skill level of workmanship was identified and experimentally evaluated to estimate the mean and standard deviation of strengths. All tested specimens were fabricated by local carpenters according to their vernacular construction practices.

The experimental methods and tests programme developed as part of this study would effectively contribute to improving current CPGU guidelines for cyclone resistance of traditional wooden houses in Madagascar and would also contribute to closing the research gap in the characterisation of the strength and behaviour of the different wooden members and connection types used for the construction of these wooden houses. One important issue related to the foundation system that was addressed and quantified is the lateral capacity of the embedded wooden column, which was revealed to be deficient when using the current practice of 50 cm (or less) embedment depth. It was shown that increasing the embedment depth to 75 cm and 100 cm increased the lateral capacity by three times and six times, respectively, of that with 50 cm embedment depth. We note that this is for sandy soil but expect similar improvements for clayey soil.

Selected results of fragility analysis are presented in this paper for a baseline structure considered representative of traditional wooden houses in the coastal regions of eastern Madagascar. In this regard, three damage states were defined for the roof system and the vertical structure system based on the performance of the building envelope. Fragility of the roof system is related to secondary member-purlin, purlin-rafter, and purlin-tie beam connections. With regards to all considered connection types, purlin-rafter connections represent the highest probability of failure with a median wind speed of 26–28 m/s. This corresponds to the severe tropical storm category on the Southwest Indian Ocean scale. Failure is due to the local construction practice in using one mid-purlin on each rafter. Increasing the number of purlins would have the benefit of reducing the purlin-rafter connections tributary area and hence lead to a reduced probability of failure. Fragility of the vertical structural system formed by the embedded columns and wall claddings revealed that, for the case of 50 cm embedded columns, the failure is always attributed to the collapse of the foundation system independently of the wall claddings connection schemes or spacing between columns. However, the case of 75 cm and 100 cm embedded columns showed damage states that are either related to the wall cladding or embedded column failures depending on the wall claddings connection schemes or spacing between embedded columns. Therefore, increasing the column embedment to 75 cm (which, notably, entails a greater time spent in excavation but no extra cost in materials), would be the single greatest improvement that could be made to improve the resilience of these structures to cyclonic wind loading. The fragility methodology discussed in this study may offer useful approaches for analysing the structural performance of traditional wooden buildings in the coastal districts of eastern Madagascar to understand and potentially reduce social and economic losses.

Declaration of Competing Interest

The authors declare that they have no known competing financial interests or personal relationships that could have appeared to influence the work reported in this paper.

Data availability

Data will be made available on request.

Acknowledgment

The work presented in this paper was funded through the Royal

Society Challenge Grant CHL\R1\180180. The authors gratefully acknowledge the *Bureau National de Gestion des Risques et des Catastrophes* (BNGRC; French for National Bureau of Risk and Disaster Management; Madagascar) for providing the cyclone-related damages data for Madagascar. In Memoriam of Prof. John Obiri for his support and help in this project. For the purpose of Open Access, the authors have applied a Creative Commons Attribution (CC BY) licence to any Author Accepted Manuscript version arising from this submission.

References

[1] Grifa C, Germinario C, Mercurio M, Izzo F, Pepe F, Bareschino P, et al. Technology, exploitation and consumption of natural resources of traditional brick productions in Madagascar. Constr Build Mater 2021;308:125022. https://doi.org/10.1016/j.conbuildmat.2021.125022.

[2] National Institute of Statistics- Instat Madagascar. Periodic Household Survey of Madagascar 2010 – Main report. Antananarivo, Madagascar, Aug. 2011. (In French).

[3] National Institute of Statistics- Instat Madagascar. Global Results of the 2018 General Census pf Population and Housing in Madagascar (RGPH-3). Antananarivo, Madagascar, Dec. 2020 (In French).

[4] National Office for Disaster and Risk Management (BNGRC). National Strategy for Risk and Disaster Management (2016-2020) in Madagascar, Oct. 2014. (In French).

[5] Stewart Mark G, Ryan Paraic C, Henderson David J, Ginger John D. Fragility analysis of roof damage to industrial buildings subject to extreme wind loading in non-cyclonic regions. Eng Struct 2016;128:333–43. https://doi.org/10.1016/j.engstruct.2016.09.053.

[6] Ben Ayed S, Aponte-Bermudez LD, Hajj MR, Tieleman HW, Gurley KR, Reinhold TA. Analysis of hurricane wind loads on low-rise structures. Eng Struct 2011;33(12):3590–6. https://doi.org/10.1016/j.engstruct.2011.07.023.

[7] Stewart Mark G, Ginger John D, Henderson David J, Ryan Paraic C. Fragility and climate impact assessment of contemporary housing roof sheeting failure due to extreme wind. Eng Struct 2018;171:464–75. https://doi.org/10.1016/j.engstruct.2018.05.125.

[8] Qin Hao, Stewart Mark G. System fragility analysis of roof cladding and trusses for Australian contemporary housing subjected to wind uplift. Struct Saf 2019;79:80–93. https://doi.org/10.1016/j.strusafe.2019.03.005.

[9] Qin Hao, Stewart Mark G. Construction defects and wind fragility assessment for metal roof failure: A Bayesian approach. Reliab Eng Syst Saf 2020;197:106777. https://doi.org/10.1016/j.ress.2019.106777.

[10] Acosta Timothy S. Risk assessment of low-rise educational buildings with wooden roof structures against severe wind loadings. Journal of Asian Architecture and Building Engineering 2022;21(3):973–85. https://doi.org/10.1080/13467581.2021.1909596.

[11] Zhang Shuoyun, Nishijima Kazuyoshi, Maruyama Takashi. Reliability-based modeling of typhoon induced wind vulnerability for residential buildings in Japan. J Wind Eng Ind Aerodyn 2014;124:68–81. https://doi.org/10.1016/j.jweia.2013.11.004.

[12] Kazuyoshi Nishijima, Chapter Ten - Housing Resilience to Wind-Induced Damage in Developing Countries, Editor(s): Emilio Bastidas-Arteaga, Mark G. Stewar, Climate Adaptation Engineering, Butterworth-Heinemann, 2019, https://doi.org/10.1016/B978-0-12-816782-3.00010-3.

[13] Rosowsky DV, Ellingwood BR. Performance-based engineering of wood frame housing: Fragility analysis methodology. J Struct Eng 2020;128(1):32–8. https://doi.org/10.1061/(ASCE)0733-9445(2004)130:12(1921).

[14] Ellingwood BR, Rosowsky DV, Li Y, Kim JH. Fragility assessment of light-frame wood construction subjected to wind and earthquake hazards. J Struct Eng 2004;130(12):1921–30. https://doi.org/10.1061/(ASCE)0733-9445(2004)130:12(1921).

[15] Lee KH, Rosowsky DV. Fragility assessment for roof sheathing failure in high wind regions. Eng Struct 2005;27(6):857–68. https://doi.org/10.1016/j.engstruct.2004.12.017.

[16] Amini MO, van de Lindt JW. Quantitative insight into rational tornado design wind speeds for residential wood-frame structures using fragility approach. J Struct Eng 204;140(7):04014033. https://doi.org/10.1061/(ASCE)ST.1943-541X.0000914.

[17] Gavanski E, Kopp GA. Fragility assessment of roof-to-wall connection failures for wood-frame houses in high winds. ASCE-ASME J Risk Uncertainty Eng Systems, Part A. Civil Engineering 2017;3(4):04017013. https://doi.org/10.1061/AJRUA6.0000916.

[18] Gill A, Genikomsou AS, Balomenos GP. Fragility assessment of wood sheathing panels and roof-to-wall connections subjected to wind loading. Front Struct Civ Eng 2021;15:867–76. https://doi.org/10.1007/s11709-021-0745-5.

[19] Kazuyoshi Nishijima, Chapter Ten - Housing Resilience to Wind-Induced Damage in Developing Countries, Editor(s): Emilio Bastidas-Arteaga, Mark G. Stewar, Climate Adaptation Engineering, Butterworth-Heinemann, 2019, https://doi.org/10.1016/B978-0-12-816782-3.00010-3.

[20] Muhammad MKA, Majid TA, Ramli NI, Deraman SNC, Wan Chik FA. An Overview of Non-Engineered Buildings Roofing System Failure under Wind Loads. Appl Mech Mater 2015;802:89–94. https://doi.org/10.4028/www.scientific.net/AMM.802.89.

[21] Kaas AC, Huang Y, Beckett CTS, Gagnon AS, Bollasina MA, Ramanantoanina H, Foster HA, McKee SM, Reynolds TPS. Cyclone vulnerability of traditional timber housing in coastal regions of Madagascar. World Conference on Timber Engineering 2021, Santiago, Chile.

[22] Knapp KR, Kruk MC, Levinson DH, Diamond HJ, Neumann CJ. The International Best Track Archive for Climate Stewardship (IBTrACS): Unifying tropical cyclone best track data. Bull Amer Meteor Soc 2010;91:363–76. https://doi.org/10.1175/2009BAMS2755.1.

[23] Knapp KR, Diamond HJ, Kossin JP, Kruk MC, Schreck CJ. 2018. International Best Track Archive for Climate Stewardship (IBTrACS) Project, Version 4. NOAA National Centres for Environmental Information. https://doi.org/10.25921/82ty-9e16 [Accessed on 10.07.2022].

[24] Joint Committee on Structural Safety (JCSS). Probabilistic model code, part 2: Loads (2001). https://www.jcss-lc.org/jcss-probabilistic-model-code/ [Accessed on 12.04.2022].

[25] Cellule de Prevention et de la Gestion des Urgences (CPGU). Guidelines for improving the cyclone resistance of traditional wooden houses. Antananarivo, Madagascar, Nov. 2016. (In French).

[26] Reason CJC, Keibel A. Tropical Cyclone Eline and Its Unusual Penetration and Impacts over the Southern African Mainland. Weather Forecast 2004;19(5):789–805. https://doi.org/10.1175/1520-0434(2004)019<0789:TCEAIU>2.0.CO;2.

[27] Probst P, Proietti C, Annunziato A, Paris S, Wania A. Tropical Cyclone ENAWO Post-Event Report. JRC Technical Reports TC-2017-000023-MDG 2017. https://doi.org/10.2760/46665.

[28] Marshall TP, Carrollton TX, Bunting WF, Weithorn JD. Procedure for Assessing Wind Damage to Wood-Framed Residences, Symposium on the F-Scale and Severe Weather Damage Assessment, CA, USA (2003).

[29] van de Lindt JW, Graettinger A, Gupta R, Skaggs T, Pryor S, Fridley KJ. Performance of Wood-Frame Structures during Hurricane Katrina. J Perform Constr Facil 2007;21(2):108–16. https://doi.org/10.1061/(ASCE)0887-3828(2007)21:2(108).

[30] Stevenson SA, Kopp GA, El Ansary AM. Framing Failures in Wood-Frame Hip Roofs under Extreme Wind Loads. Front Built Environ 2018;4:6. https://doi.org/10.3389/fbuil.2018.00006.

[31] Parker JW, Good JP. Madagascar: Training for Safer Construction after cyclone Kamisy - Case study as part of the project- Evaluation of Post-Disaster Housing Education as a Local Mitigation Approach. AID Office of U.S. Foreign Disaster Assistance, Washington, USA (1993).

[32] Ralijoana MA, Critical analysis of anti-cyclones constructions regulation in Madagascar. DESS degree dissertation. Faculty of Law, Management Economics and Sociology, University of Antananarivo, 2011 (In French).

[33] Xiaowei L, Junhai Z, Guowei M, Shuanghua H. Experimental Study on the Traditional Timber Mortise-Tenon Joints. Adv Struct Eng 2015;18(12):2089–102. https://doi.org/10.1260/1369-4332.18.12.2089.

[34] Xie Q, Wang L, Zheng P, Zhang L, Hu W. Rotational behaviour of degraded traditional mortise-tenon joints: experimental tests and hysteretic model. Int J Archit Heritage 2018;12(1):125–36. https://doi.org/10.1080/15583058.2017.1390629.

[35] Linlin M, Xue J, Dai W, Zhang X, Zhao X. Moment-rotation relationship of mortise-through-tenon connections in historic timber structures. Constr Build Mater 2020;232:117285. https://doi.org/10.1016/j.conbuildmat.2019.117285.

[36] Bowling T. Simplified analysis of laterally loaded posts. Austr Geomech J 2011;46(1).

[37] European Committee for Standardization, Eurocode 1: Actions on structures — Part 1-4: General actions — Wind Actions. (2005).

[38] Gulvanessian H, Holicky M. Eurocodes: using reliability analysis to combine action effects. Proc Inst Civ Eng: Struct Build 2005;158(4):243–52. https://doi.org/10.1680/stbu.2005.158.4.243.